A MICROGRID CONTROL FOR DC WIND POWER GENERATION USING ANN

[1]P.Manoj Kumar,[2]Dr.V.Praveen,[3]K.Narendra
[1]Associate Professor, PSCMRCET
[2]Associate Professor, PSCMRCET
[3]Assistant Professor, PSCMRCET
([1]pmanoj249@gmail.com,[2]praveenveceee@gmail.com,[3]nano.knk@gmail.com)

Abstract— In this paper, the strategy of ANN controller is proposed with DC grid based wind power generation system. The proposed system permits the flexible operation of multiple parallel connected wind generators without the need of voltage and frequency synchronization. A control scheme which uses separate controllers for the inverters during grid-connected and islanded operation is proposed. For the control of inverters, a model predictive algorithm is proposed for the better transient response with respect to the changes in the operating conditions. ANN is a non-linear model that is easy to use and understand compared to statistical methods. ANN is non-parametric model while most of statistical methods are parametric model that need higher background of statistic. To increase the controller's robustness against variations in the operating conditions ANN based controller is introduced. The fluctuations of the micro grid are controlled with the constant regulated power a separate controller is introduced to the wind power to maintain the fixed power to mitigate the variational errors. To demonstrate the operational capability of the proposed micro grid when it operates connected to and islanded from the distribution grid, and the results obtained are discussed.

Keywords—Wind generation;dc grid;energy management;model predictive control (key words)

I.   INTRODUCTION

In general, for the production of power renewable energy sources are most popular and fast increasing now-a-day. To reduce the farms demand on the grid, wind power is generated. Poultry farming is the raising of domesticated birds for the purpose of farming for the food (meat or eggs). To ensure that the poultries remain productive, the poultry farms are required to be maintained at comfortable temperature. The cooling fans with tens of kilowatt are installed to regulate the farms demand on the grid [1]- [3]. The wind energy produced by cooling fans are not only used for the cooling the farms but also can be harnessed by using the wind turbines to reduce the farms demand on the grid [4]. The major difference between the poultry farms and the conventional wind farms is the wind speed variability. The wind speed in the conventional wind farms is variable, whereas in the poultry farms it is constant. Thus, the generation periodic issues that affect the reliability of the electricity and power balance are not extensive in the poultry farm wind energy system.

Many research works have been conducted to facilitate the integration of DERs and energy storage devices in dc micro grids. A dc microgrid consisting of a matrix converter, high frequency transformer and a single phase ac/dc converter is proposed in [5], [6]. The WTs are clustered into four groups and each one is connected to a converter is proposed in [7]-[10]. A hybrid ac/dc wind farm architecture consists of a both ac and dc networks connected by a bidirectional converter is proposed in [11], [12]. To design the controllers for the inverters to operate in grid connected and islanded operation is conducted in [13]- [15]. The MPC scheme with modulation techniques or cascaded control loops is proposed in [16]. The usefulness of MPC scheme for the control of different converters is investigated in [17]. MPC models predict the changes in the dependent variables of the modeled system that will be caused by changes in the independent variables. As compared to the control methods MPC algorithm allows the specific performance which is close to the limits in handling the constraints [18]- [19]. The MPC control scheme for the control of inverters is proposed in detail [20]- [22].

II.   EXSISTING SYSTEM

A. System Description

The overall configuration of dc grid based wind power generation system in a poultry farm is shown in the Fig.1.The system operates either connected to or islanded from the distributed grid and the system consists of four 10kw permanent magnet synchronous generators(PMSGs) which are driven by the variable speed WTs. The design complexity of the control hardware is reduced by using the PMSGs because it does not need any dc excitation system. The three phase output of the each PMSG is given to the three phase rectifier (i.e., converters A, B, C and D) in order to maintain the dc output voltage of the each PMSG to the level want to be at the dc grid. The total power at the dc grid is inverted by the two inverters (i.e., inverters1and2) rated of 40kW. The two inverters are used between the dc grid and the ac grid is proposed instead of using the individual inverters. This structure reduces the need to synchronize the voltage, frequency and phase, and provides the flexible operation of the wind generators plug in and off with the minimum disturbances in the dc grid.

The converters and the inverters are coordinated by the energy management system which regulates and controls the power imbalance by the each WG and the load power consumption through the centralized server. The output voltages of the inverters (1 & 2) are to be maintained same

through the EMS to prevent the excessive circulating currents between the two inverters.

During normal operation, the two inverters will share the output from the PMSGs (i.e., each inverter shares 20kW). The maximum power generated by the each WT is estimated from the optimal wind power $P_{wt,opt}$ as follows [23].

$$P_{wt,opt} = k_{opt}(\omega r, opt)^3 \tag{1}$$

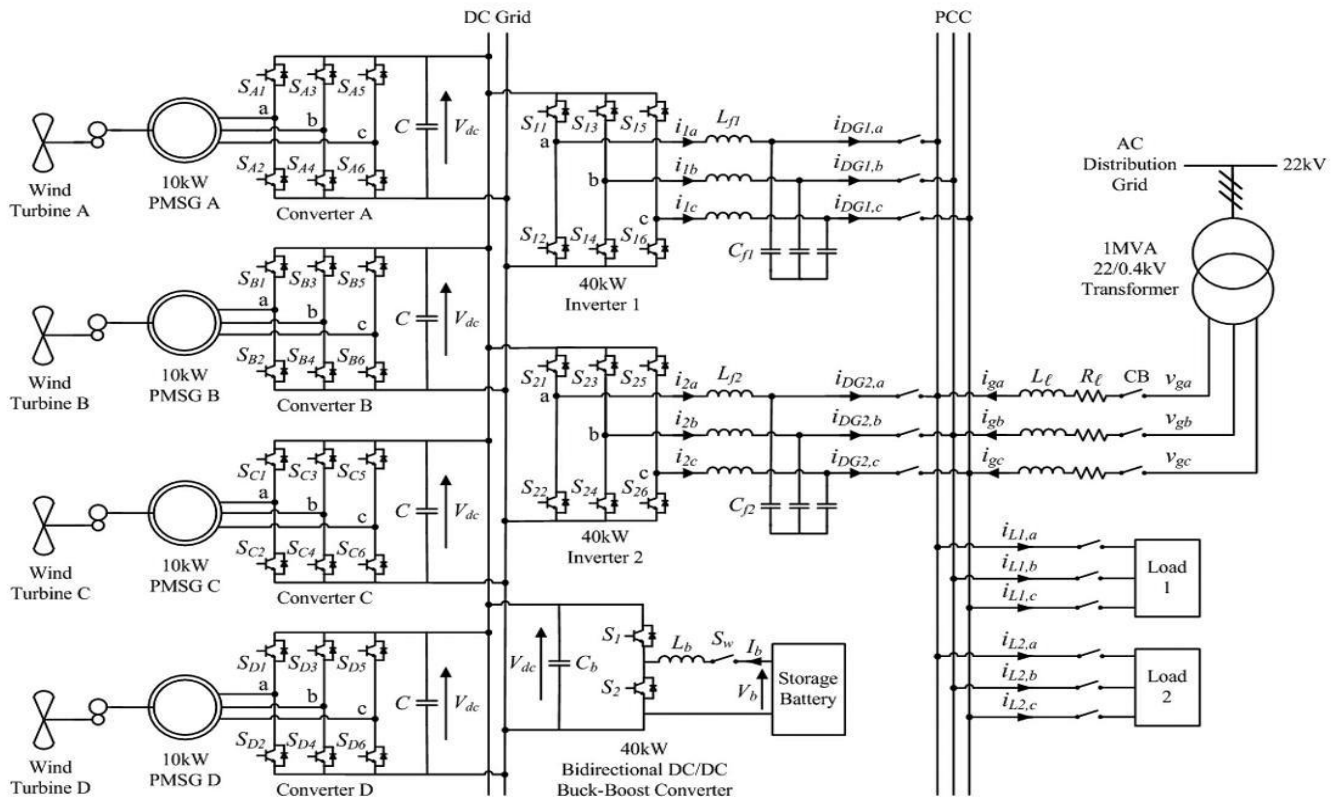$$K_{opt} = \frac{1}{2}C_{p,opt}\, \rho A \left(\frac{R}{\lambda_{opt}}\right)^3 \tag{2}$$

Fig.1:Overall configuration of proposed dc grid based wind power generation system in a microgrid

$$\omega r, opt = \frac{\lambda_{opt}\, V}{R} \tag{3}$$

where k_{opt} is the optimized constant, $\omega_{r,opt}$ is the wind turbine speed for optimum power generation, $C_{p,opt}$ is the optimum power coefficient of the turbine, ρ is the air density, A is the area swept by the rotor blades, λ_{opt} is the optimum tip speed ratio, v is the wind speed and R is the radius of the blade.

When one inverter is fails to operate or is under maintenance, the maximum of 40kW of output power from the PMSGs is handled by the other inverter alone. Hence the proposed tropology provides the increased reliability and ensure the continuous operation, when either inverter 1 or inverter 2 is disconnected from operation.

When the microgrid operates connected or islanded from the grid, an 80Ah storage battery (SB) which is sized according to [24], to facilitate the charging and discharging operations through the bidirectional ac/dc 40kW buck-book converter is

connected. In the proposed dc grid, the energy conditions of the storage battery (SB) are determined based on the system-on-a-chip (SOC) limits given by

$$SOC_{min} < SOC \leq SOC_{max} \tag{4}$$

SB swiftly monitors the voltage at the dc grid, and reduces the effect of fluctuations in the power generation and the load demand by charging during the off-peak loads and by discharging when the load on the grid is high.

B. System Operation

When the microgrid is connected to the distributed grid, the WTs are responsible for the power delivered to the loads, thereby to reduce the load demand on the grid. SB is used to control the demand side management functions.

During islanded operation, the WTs and the SB is the only sources to supply the load demand on the grid. The SB can

supply the power for the deficit of power imbalance in the microgrid as given below,

$$P_{wt} + P_{sb} = P_{loss} + P_l$$

Where P_{wt} is the real power delivered by the WT, P_{sb} is the real power supplied by the SB which is subjected to the maximum power condition during the discharging and is given by,

$$P_{sb} \leq P_{sb,max}$$

P_l is the real power supplied to the loads, P_{loss} is the system loss

C. AC/DC Converter Modeling

Fig.2. shows the power circuit of ac/dc converter which is connected to the three phase PMSG. The balanced three phase ac voltage sources of the PMSGs are e_{sa}, e_{sb}, and e_{sc} with the resistance R_S and the inductance L_S respectively [30], [31]. The PMSG currents i_{sa}, i_{sb}, i_{sc} and the output voltage V_{dc} of the converter and their state equations are as follows:
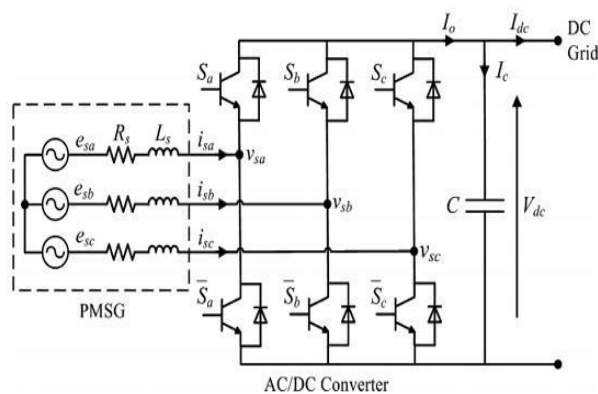

Fig.2:Power circuit of a PMSG connected to an ac/dc voltage source converter.

$$L_s\frac{di_s}{dt} = -R_s\, i_s + e_s - KSV_{dc} \qquad (7)$$

$$C\frac{dV_{dc}}{dt} = i_s^T S - I_{dc} \qquad (8)$$

$$i_s = \begin{bmatrix} i_{sa} & i_{sb} & i_{sc} \end{bmatrix}^T, \quad e_s = \begin{bmatrix} e_{sa} & e_{sb} & e_{sc} \end{bmatrix}^T$$

$$K = \begin{bmatrix} 2/3 & -1/3 & -1/3 \\ -1/3 & 2/3 & -1/3 \\ -1/3 & -1/3 & 2/3 \end{bmatrix}$$

$S = \begin{bmatrix} S_a & S_b & S_c \end{bmatrix}^T$ is the ac/dc converter switching functions which are defined as

$$S_j = \begin{cases} -x, & S_j \text{ is ON} \\ x, & S_j \text{ is OFF} \end{cases} \quad \text{for } j = a,b,c \qquad (9)$$

D. DC/AC Inverter Modeling

The two inverters which are connected between the dc grid and the point of common coupling are identical. The single phase representation of the DC/AC inverter is shown in the Fig.4. The Kirchhoff's voltage current laws are applied to the loop I and the point x respectively, to derive the state space model of the DC/AC inverter and the equations obtained are:

$$L_f\frac{di}{dt} + iR + v_{DG} = uV_{dc} \qquad (10)$$

$$i_{DG} = i - i_{cf} \qquad (11)$$

where V_{dc} is the voltage of the dc grid, u is the control signal, R is the inverter loss, L_f and C_f are the inductance and capacitance of the low-pass (LPF) filter respectively, i_{DG} is the output current of the inverter, i is the current flowing through L_f, i_{Cf} is the current flowing through C_f, v_{DG} is the inverter output voltage
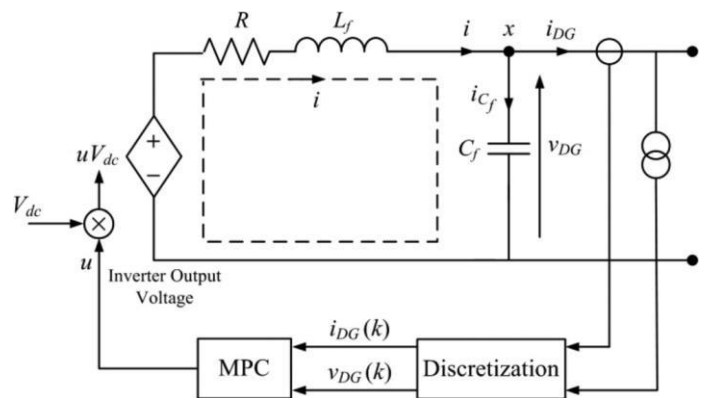

Fig.3: Single phase representation of the three phase dc/ac inverter

During grid connected operation, the inverters are operated in current control mode (CCM) because the frequency and magnitude of the output voltage are tied to the grid voltage. Thus the state space equations for the inverter can be expressed with the sampling time Ts as follows:

$$X_g(k + 1) = A_g x_g(k) + B_{g1} v_g(k) + B_{g2} u_g(k) \qquad (12)$$

$$Y_g(k) = C_g x_g(k) + D_g v_g(k) \qquad (13)$$

Where the subscript g represents the inverter model during grid connected operation, k is the discretized present time step, and

$$A_g = 1 - \frac{R}{L_f}T_s, \quad B_{g1} = \begin{bmatrix} 0 & -\frac{T_s}{L_f} \end{bmatrix}, \quad B_{g2} = \frac{V_{dc}}{L_f}T_s,$$

$$C_g = 1, \quad D_g = \begin{bmatrix} \frac{C_f}{T_s} & -\frac{C_f}{T_s} \end{bmatrix}$$

$x_g(k) = i(k)$ is the state vector, $v_g(k) = [v_{DG}(k+1)\ v_{DG}(k)]^T$ is the exogenous input; $u_g(k)$ is the control signal with $-1 \leq u_g(k) \leq 1$; and $y_g(k) = i_{DG}(k)$ is the output. The

exogenous input $v_g(k)$ can be calculated using state estimation. A three phase sinusoidal signal is directly given as the exogenous input, when it is operating in CCM.

The inverters will be operating in the voltage control mode(VCM) during islanded operation. The rate of change of the input output current is much slower when compared to T_S. Hence the following assumption is made when deriving the state space equations for the inverter operating in the VCM [33]:

$$\frac{diDG}{dt} = 0 \qquad (14)$$

Considering the above assumption, the state space equation for the inverter operating in the VCM can be expressed as:

$$x_i \,(k+1) = A_i x_i(k) + B_i u_i(k) \qquad (15)$$

$$y_i \,(k) = C_i \, x_i \,(k) \qquad (16)$$

where the subscript i represents model inverter model during grid disconnected from the distributed grid operation and

$$A_i = \begin{bmatrix} 1 - \frac{R}{Lf} Ts & -\frac{Ts}{Lf} & 0 \\ \frac{Ts}{Lf} & 1 & -\frac{Ts}{Cf} \\ 0 & 0 & 1 \end{bmatrix},$$

$$B_i = \begin{bmatrix} \frac{Vdc}{Lf} Ts & 0 & 0 \end{bmatrix}, \; C_i = \begin{bmatrix} 0 & 1 & 0 \end{bmatrix}$$

$x_i(k) = [i(k) \; vDG(k) \; iDG(k)]^T$ is the state vector; $u_i(k)$ is the control signal with $-1 \le u_i(k) \le 1$; and $y_i(k) = vDG(k)$ is the output. The inverters are essential to deliver the offered power from the PMSGs to stream the loads, during islanded operation. Hence the output voltage is maintained and the output current is determined from the total power.

E. Control Design for DC/AC Inverter

In both grid connected and islanded operation ,a model based control using the model predictive control is used to control the inverters. MPC adopts a receding horizon approach in which the optimization algorithm will compute a sequence of control actions to the minimum seleative objectives in the whole control horizon approach.The inverter executes the first control action only.This gives the better transient response when compared to the other PI/PR controllers.The state space equations are transformed into the argumented state space euations by using the incremental variables for the inverter.

$$\Delta \xi(k) = \xi(k) - \xi(k-1) \qquad (17)$$

where ξ represents each variable in the inverter model, such as

vDG, iDG, i and u as shown in Fig.4. By describing the incremental variables, the improved state space model for the inverter model operating in the CCM during grid-connected operation can be expressed as follows:

$$X_g(k+1) = A_{g\_aug}X_g(k) + B_{g1\_aug}V_g(k) + B_{g2\text{-}aug}U_g(k) \qquad (18)$$

$$Y_g(k) = C_{g\_aug}X_g \,(k) \qquad (19)$$

Where,

$$A_{g\_aug} = \begin{bmatrix} 1 - \frac{R}{Lf} Ts & 0 \\ 1 - \frac{R}{Lf} Ts & 1 \end{bmatrix}$$

$$B_{g1\_aug} = \begin{bmatrix} 0 & 0 & -\frac{Ts}{Lf} \\ -\frac{Cf}{Ts} & \frac{Cf}{Ts} & -\frac{Ts}{Lf} \end{bmatrix}$$

$$B_{g2\_aug} = \begin{bmatrix} \frac{Vdc}{Lf}Ts & -\frac{Vdc}{Lf}Ts \\ \frac{Vdc}{Lf}Ts & -\frac{Vdc}{Lf}Ts \end{bmatrix}$$

$$C_{g\_aug} = \begin{bmatrix} 0 & 1 \end{bmatrix}$$

$X_g \,(k) = [\Delta i(k) \; iDG(k)]^T$ is the state vector; $V_g(k) = [\Delta vDG(k + 2) \; \Delta vDG(k + 1) \; \Delta vDG(k]^T$ is the exogenous input; $U_g(k) = \Delta u_g(k)$ is the control signal; and $Y_g(k) = iDG(k)$ is the output. Similarly the agumented state space equation for the inverter model operating in the VCM model as follows:

$$X_i(k+1) = A_{i\_aug}X_g(k) + B_{i\_aug}U_i(k) \qquad (20)$$

$$Y_i \,(k) = C_{i\_aug} \, X_i \,(k) \qquad (21)$$

Where,

$$A_{i\_aug} = \begin{bmatrix} 1 - \frac{R}{L_f}T_s & -\frac{T_s}{L_f} & 0 & 0 \\ \frac{T_s}{L_f} & 1 & -\frac{T_s}{L_f} & 0 \\ 0 & 0 & 1 & 0 \\ \frac{T_s}{L_f} & 1 & \frac{T_s}{L_f} & 1 \end{bmatrix},$$

$$B_{i\_aug} = \begin{bmatrix} \frac{V_{dc}}{L_f}T_s \\ 0 \\ 0 \\ 0 \end{bmatrix}, \; C_{i\_aug} = \begin{bmatrix} 0 & 0 & 0 & 1 \end{bmatrix}$$

$X_i(k) = [\Delta i(k) \; \Delta vDG(k) \; \Delta iDG(k) \; vDG(k)]^T$ is the state vector;

$U_i(k) = \Delta u_i(k)$ is the control signal; and $Y_i(k) = vDG(k)$ is the output.In the MPC algorithm ,a cost function is solved using quadratic equation for the control of inverters in both CCM and VCM model [33]:

$$J = (Rs - Yj)^T(Rs - Yj) + Uj^T QUj \qquad (22)$$

subject to the limitation

$$-1 \le u_j(k) \le 1 \qquad (23)$$

Where Rs is the set point matrix; Q is the tunning matrix for the desired closed loop performance, Yj is the output of either the augmented model in the CCM or VCM (i.e., Yg or Yi), Uj is the control signal of either the augmented model in the CCM or VCM (i.e., Ug or Ui). The first part of the cost

function compares the output of the augmented Yi with the reference and to ensure the output tracks with the minimum error. The second part of the cost function is to calculate the weighted factor of the control signal and to maintain the MPC algorithm within the limits. After the control signal u is generated by the MPC algorithm, it will be applied to the dc/ac inverter as shown in Fig. 3.

F. Artificial Neural Network

Neural –Networks is one of those words that is getting fashionable in the new era of technology. Just as there is a biological neuron, there is a basic artificial neuron. Each neuron has a certain number of inputs, each of which have a weight assigned to them.

Each neuron has its own unique threshold value, and it the net is greater than the threshold, the neuron fires (or outputs a 1), otherwise it stays quiet (outputs a 0). The output is then fed into all the neurons it is connected to. ANN have many different coefficients, which it can optimize. Hence, it can handle much more variability as compared to traditional models.

The neurons in an ANN are arranged into layers. Using supplementary layers of hidden neurons allows greater processing power and system flexibility. This surplus flexibility originates at the cost of additional complexity in the training algorithm. Neuron consisting of few hidden layers reduces the robustness of the system. The more hidden layers in the neuron increase the complexity in the training algorithm.

ANNs have three layers that are interconnected. The first layer consists of input neurons. Those neurons send data on to the second layer, which in turn sends the output neurons to the third layer

While there is a fair understanding of how an individual neuron works, there is still a great deal of research and mostly conjecture regarding the way neurons organize themselves and the mechanisms used by arrays of neurons to adapt their behavior to external stimuli. There are a large number of experimental neural network structures currently in use reflecting this state of continuing research.
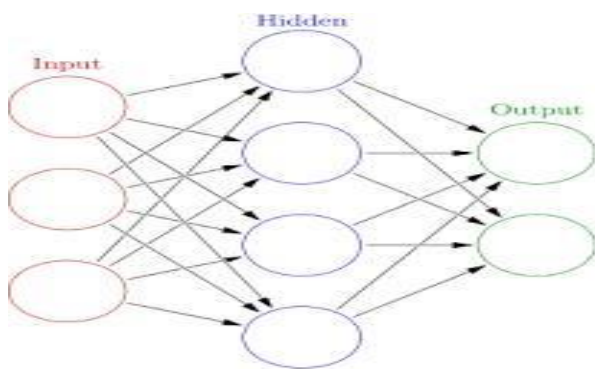

Fig.4: Artificial Neural Network

In between the input units and output units are one or more layers of hidden units, which, together, form the majority of the artificial brain. Most neural networks are fully connected,

which means each hidden unit and each output unit is connected to every unit in the layers either side.

The neuron will combine these weighted inputs and, with reference to a threshold value and activation function, use these to determine its output. This behavior follows closely our understanding of how real neurons work.
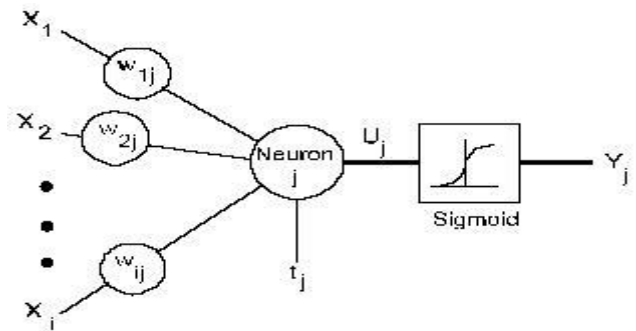

Fig.5: A Model Neuron

The advances in this field will increase their popularity. They are excellent as pattern classifiers/recognizers – and can be used where traditional techniques do not work. Neural-Networks can handle exceptions and abnormal input data, very important for systems that handle a wide range of data.

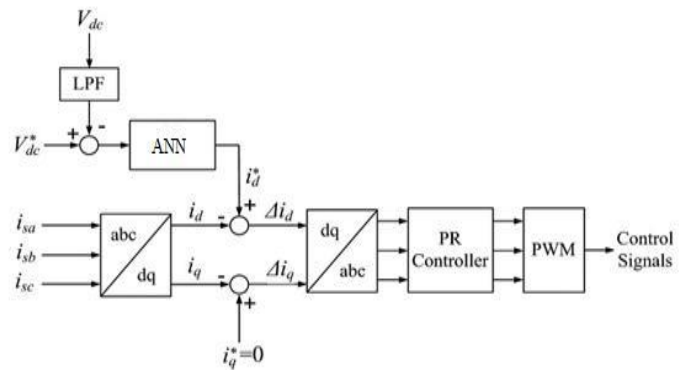*G. Control Design   for AC/DC converter*

Fig.6:Configuration of proposed controller for ac/dc converter.

Fig. 5 shows the configuration of proposed controller for ac/dc converter which is employed to maintain the output

voltage V_{dc} of each converter. It compensates the fluctuations

the V_{dc} due to the power dissimilarities in the dc grid. The high frequency switching wrinkles are disregarded via

circulating the V_{dc} first into the low pass filter (LPF). Then the Vdc is fed into the artificial neural network to generate the

`current reference i_d^* for id to track. The artificial neural network makes number of iterations to reduce the robustness of the system. The current errors are then converted into the abc frame to reduce the more fluctuations and then it is fed into the proportional resonant controller to generate the

required control signals by utilizing the pulse width modulation technique.

By using the artificial neural network, the better transient response will be obtained when compared with the other PI/PR controllers. The more number of iterations which was done in the hidden layers by comparing the more values to obtain the required output. ANN reduces the time delay to track the references in the initialization period. Hence the maximum power can be obtained in the less time.

III. NUMERICAL ANALYSIS

The Simulink model of a proposed dc grid based wind power generation system is as shown in the Fig.1 in the MATLAB/SIMULINK. The effectiveness of the proposed design concept is estimated under different operating conditions when the dc grid is connected or islanded from the distribution grid. The impedances of the distribution lines are obtained in [33]. The table.1 represents the system parameters. In practical implementations, the values of the inverter loss resistance and the converter are not exactly known. Hence the values are coarsely estimated.

Parameter	Value
Distribution grid voltage	Vg = 230V(phase)
DC grid voltage	Vdc = 500V
PMSG stator impedance	Rs = 0.2 Ω,Ls = 2.4 mH
Distribution line impedance	Rl = 7.5mΩ,Ll = 25.7μH
Inverter LC filter	Lf = 1.2mH,Cf = 20μF
Converter capacitor	C = 300μF
Converter and Inverter loss resistance	R = 1mΩ
Load 1 rating	P_{L1} = 35kW,Q_{L1}=8kVAr
Load 2 rating	P_{L2} = 25kW,Q_{L2}=4kVAr

Table.1: Parameters of the system

A. Test Case 1:Faliure of One Inverter During Grid - Connected operation

When the micro grid is connected to the distributed grid, the proposed wind power generation system will supply to reach part of the load demand. Under normal operating conditions, the total power generated by the four PMSGs is to be converted by the two inverters which will share the total power supplied to the loads. If one inverter fails, then the total power will be inverted by the other inverter which is rated of 40kW.

Each PMSG generating about 5.5kW of real power, the total real power generated by the four PMSGs are about 22kW which is converted by the inverters 1 and 2 is 20kW of real power and 8kVAR of reactive power respectively.
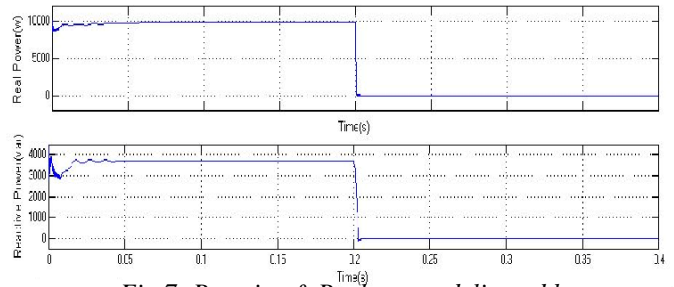

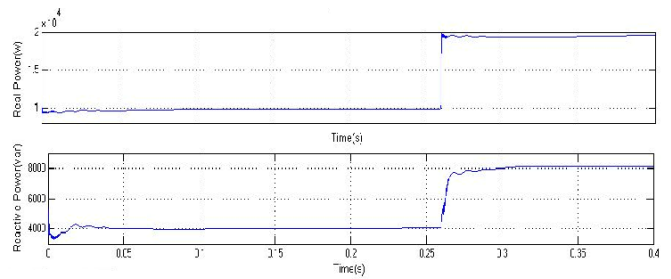*Fig.7: Reactive & Real power delivered by inverter 1*

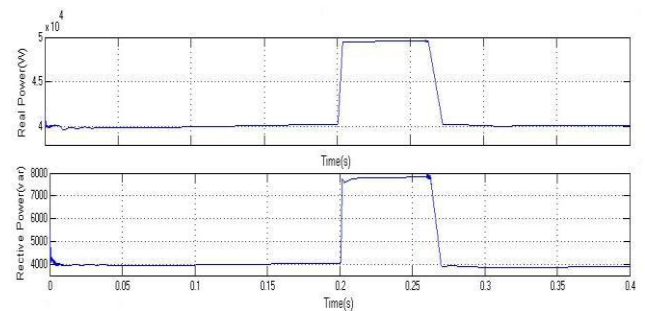*Fig.8: Reactive & Real power delivered by inverter 2*

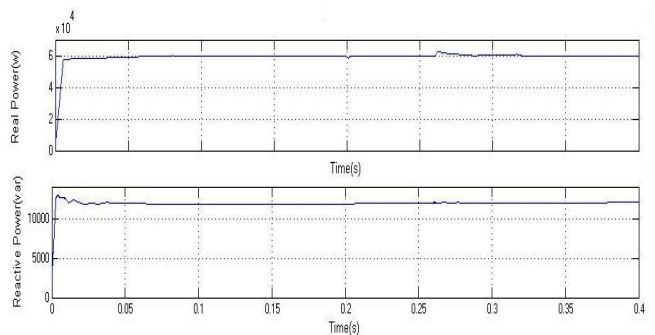*Fig .9: Reactive & Real power delivered by the grid*

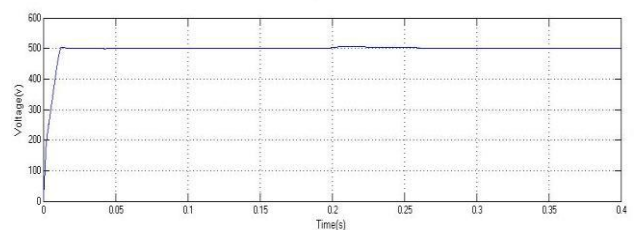*Fig .10: Reactive & Real power consumed by the loads*

Fig .11: DC Grid Voltage

Fig 7 and 8 shows the real and reactive power delivered by the inverter 1and 2 for 0 ≤ t < 0.2s respectively. For 0 ≤ t < 0.2s, both the inverters deliver 10kW and 4kVAR of real and reactive power to the loads. The remaining power is delivered by the grid to the loads is shown in the Fig 9. The grid delivers 40kW of real power and 4kVAR of reactive power to the loads during the time period 0 ≤ t < 0.2s. Fig 10 shows the total real and reactive power consumed the loads is about 60kW and 12 kVAR.

At t=0.2s the inverter 1fails to operate, then the power loss of 10kW of real power and 4kVAR of reactive power supplied to the loads. To the loss of inverter 1, the delay of three cycles is introduced to cater for the response of EMS. The inverter 2 increases to 20kW of real and 8kVAR of reactive power to the loads, as shown in the Fig 13. By using the ANN controller, the time period required by the controller to track references will be reduced compared to the other controllers. MPC algorithm is able to quickly track the power references as compared to the conventional control strategies.

B. Test Case 2: AC/DC Converter during Grid-Connected Operation

In this mode, the PMSG A is disconnected at t=0.2s hence the power loss occurred will be compensated by the distribution grid by increasing the real and reactive power supplied to the loads. The most significant advantage of the proposed dc grid based wind power generation system is to facilitate the connection of any PMSGs without the need of voltage and frequency synchronization.
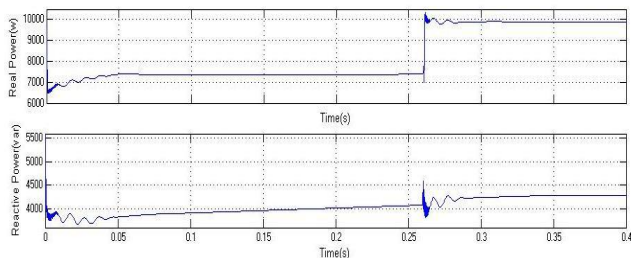

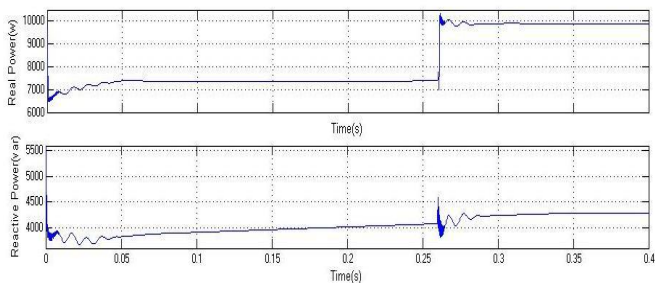*Fig .12: Reactive & Real power delivered by inverter 1*
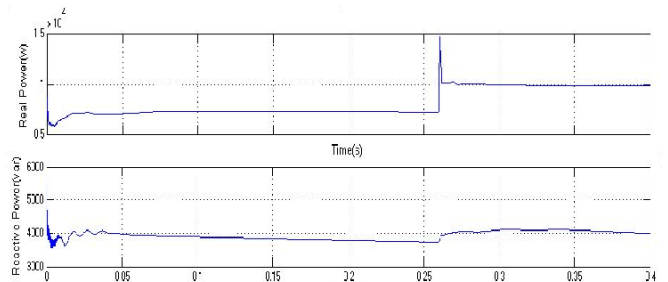

Fig .13: Reactive & Real power delivered by inverter 2

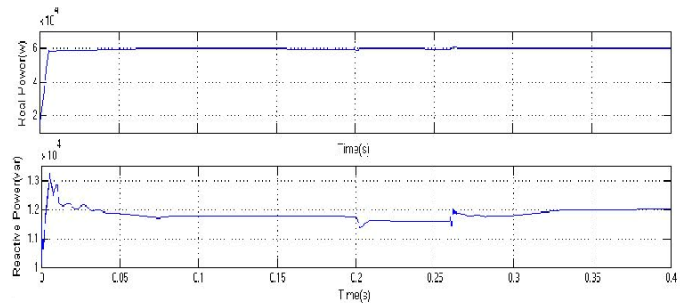*Fig. 14: Reactive & Real power consumed by the loads*

Fig. 15: Reactive & Real power delivered by the grid

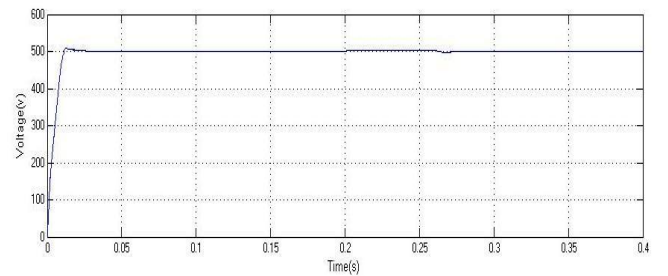*Fig .16:DC Grid Voltage*

The microgrid is operating the grid connected mode, the PMSG A is disconnected from the grid for 0<t< 0.2s. Hence the power loss is delivered by the grid, to meet the loads demand on the grid. The remaining three PMSGs delivers the power of 16kw of real power and 4kVAR of reactive power which was converted by the two inverters into 14kW and 8kVAR of real and reactive powers to the loads. The remaining power was delivered by the grid in the time period of 0.26 < t < 0.4s. The grid delivers the real power of 46kW until 0 < t < 0.2s, for t=o.26s the grid delivers the 40 kW. This cause the dip in the voltage waveforms of the grid at t=0.2s. For t=0.26s the grid voltage is again reaches to its normal value of 500V.

By using the ANN controller, the fluctuations in the waveforms is reduced and the time delay to track the references is also being reduced. Hence the total harmonic distortion of the waveforms is also being reduced. ANN controller increases the robustness of the system.

C. Test case 3: Islanded Operation

In this case the micro grid is disconnected from the distribution grid due to the fault occurrence; hence the grid is

disconnected by the circuit breakers. Therefore, the power delivered by the distribution grid is compensated by the storage battery. During grid connected operation the storage battery will charge and in islanded operation it will discharge.

Fig .17: Reactive & Real power delivered by inverter 1

Fig .18: Reactive & Real power delivered by inverter 2

Fig. 19:Reactive & Real power delivered by grid.

Fig .20: Power & Voltage delivered by DC Grid and Storage Battery

Initially the micro grid is operating in grid connected mode then the grid is supplying of real power 40kW and reactive power of 4kVAR to the loads for $0 \leq t < 0.2s$. The two inverters deliver the real and reactive power of 10kW and 4kVAR respectively. At t=0.2s the grid is disconnected from the

distribution grid due to the fault occurred in the upstream network of the distribution grid. The SB is employed by EMS to maintain the stability of the microgrid by supplying the 40kW and 4kVAR to the loads.

At the same time, the inverters deliver the real and reactive power of 30kW and 8kVAR. Therefore, the voltage dip in the dc grid voltage is observed in the waveforms.
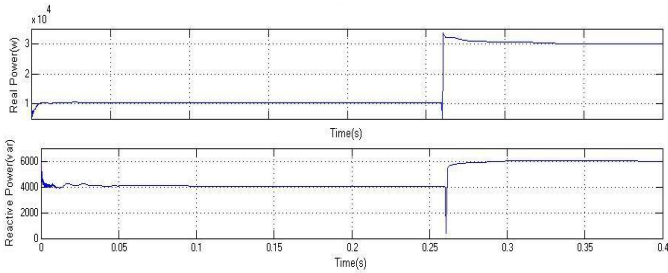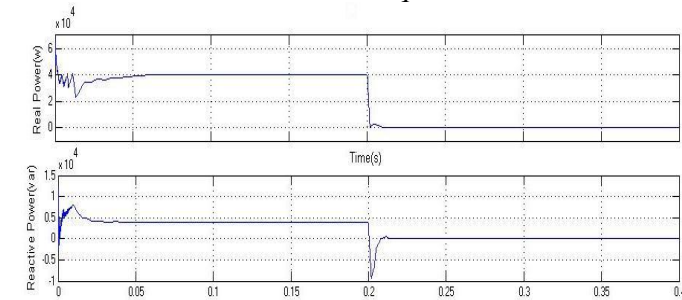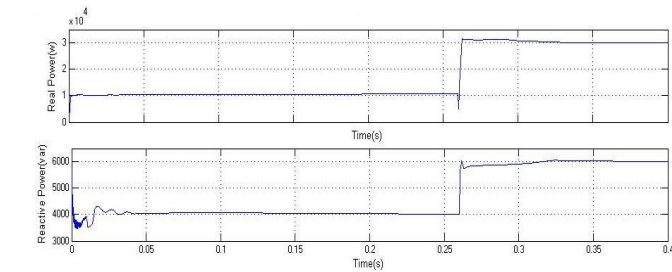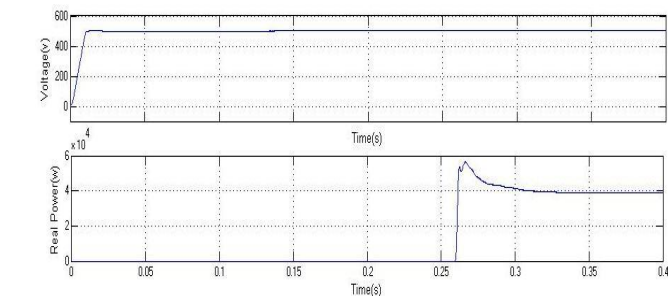
IV. TOTAL HARMONIC DISTORTION

The total harmonic distortion, or THD, of a signal is a measurement of the harmonic distortion present and is defined as the ratio of the sum of the powers of all harmonic components to the power of the fundamental frequency. THD is used to characterize the linearity of audio systems and the power quality of electric power systems. Distortion factor is a closely related term, sometimes used as a synonym. The measurement is the most commonly defined as the ratio of the RMS amplitude of a set of higher harmonic frequencies to the RMs amplitude of the first harmonic, or fundamental frequency:

$$THD = \frac{\sqrt{(V2^2 + V3^2 + V4^2 + \cdots)}}{V1}$$

Where V_n is the RMS voltage of the nth harmonic and n=1 is the fundamental frequency
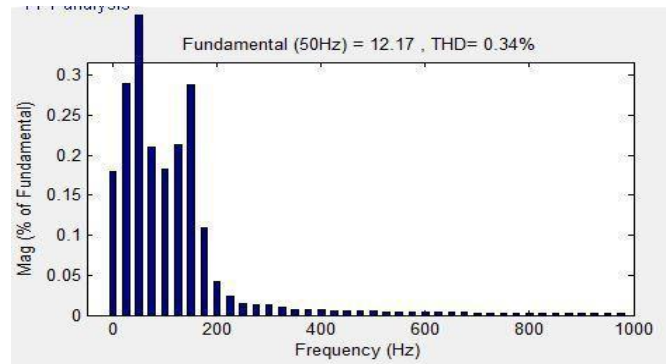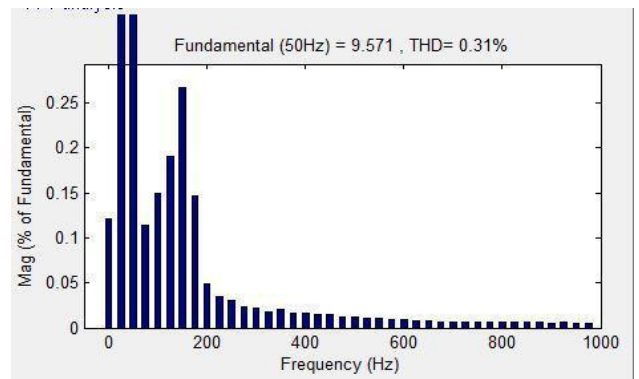

Fig .21: THD of DC grid1

Fig .22: THD of DC grid2
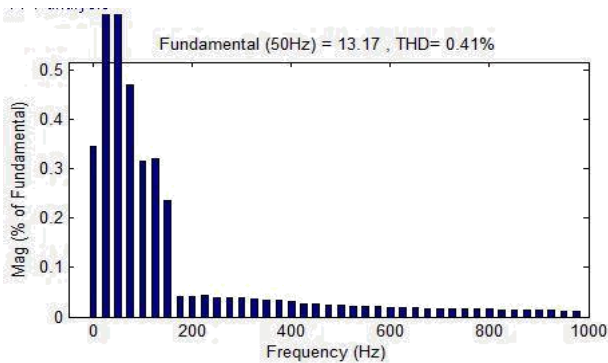
Fundamental (50Hz) = 13.17 , THD= 0.41%

Fig. 23:THD of DC grid3

The above three Fig 21,22 and 23 shows the harmonic distortion of dc grid based wind power generation system in a microgrid in three different cases, when the grid is connected to or islanded from the distribution grid. The values of improved harmonic distortion of dc grid based wind power generation system can be obtained as follows 0.34%, 0.31%, and 0.41%, during the grid connected or islanded mode of operation.

V.   CONCULSION

In this paper, the design of ANN control of dc grid based wind power generation system in a micro grid that facilitates the several WGs to be operated in parallel in a poultry farm has been introduced. In the micro grid operation, the proposed design eliminates the need for voltage, frequency and phase synchronization as compared to the conventional wind power generation systems, thus allowing the WGs to be switched on or off with minimal disturbances. The design concept has been verified through various test scenarios to determine the operational ability of the suggested micro grid and thus the design concept offer the improved flexibility and reliability in the simulation results has shown. However the design concept requires further experimental validation to reduce the measurement errors due to the inaccuracies. The improved results can be obtained when compared to the other controllers. The simulation results obtained and the analysis obtained can be used for the design of the dc grid based wind power generation system.

REFERENCES

[1]   K. T. Tan, B. Sivaneasan, X. Y. Peng, P. L. So ―Control and Operation of a DC Grid-Based Wind Power Generation System in a Microgrid, IEEE Transection on Energy Conservation, vol. 31, no. 2, June 2016

[2]   M.CzarickandJ.Worley,―Windturbinesandtunnelfans, PoultryHousing Tips, vol. 22, no. 7, pp. 1–2, Jun. 2010.

[3]   The poultry guide: Environmentally control poultry farm ventilation systems for broiler, layer, breeders and top suppliers. [Online]. Available: http://thepoultryguide.com/poultry-ventilation/

[4]   Livestock and climate change. [Online]. Available: http://www. worldwatch.org/files/pdf/Livestock%20and%20Climate%20Change. pdf.

[5]FarmEnergy:Energyefficientfansforpoultryproduction.[Online].Av ailable: http://farmenergy.exnet.iastate.edu.

[6]   A. Mogstad, M. Molinas, P. Olsen, and R. Nilsen, ―A power conversion system for offshore wind parks in Proc. 34th IEEE Ind. Electron., 2008, pp. 2106–2112.

[7]   A. Mogstad and M. Molinas, ―Power collection and integration on the electric grid from offshore wind parks in Proc. Nordic Workshop Power Ind. Electron., 2008, pp. 1–8.

[8]   D. Jovic, ―Offshore wind farm with a series multiterminal CSI HVDC, Elect. Power Syst. Res., vol. 78, no. 4, pp. 747–755, Apr. 2008.

[9]   X.Lu,J.M.Guerrero,K.Sun,andJ.CVasquez―Animproveddr oopcontrol method for DC microgrids based on low bandwidth communication with DC bus voltage restoration and enhanced current sharing accuracy, IEEE Trans. Power Electron., vol. 29, no. 4, pp. 1800–1812, Apr. 2014.

[10]   T. Dragicevi, J. M. Guerrero, and J. C Vasquez, ―A distributed control strategy for coordination of an autonomous LVDC microgrid based on power-line signaling, IEEE Trans. Ind. Electron., vol. 61, no. 7, pp. 3313– 3326, Jul. 2014.

[11]   N. L. Diaz, T. Dragicevi, J. C. Vasquez, and J. M. Guerrero, ―Intelligent distributed generation and storage units for DC microgrids—A new concept on cooperative control without communications beyond droop control IEEE Trans. Smart Grid, vol. 5, no. 5, pp. 2476–2485, Sep. 2014.

[12]   X. Liu, P. Wang, and P. C. Loh, ―A hybrid AC/DC microgrid and its coordinationcontrol, IEEETrans.SmartGrid,vol.2,no.2,pp.278–286,   Jun. 2011.

[13]   J. A. P. Lopes, C. L. Moreira, and A. G.Madureira, ―Defining control strategies for microgrids islanded operation, IEEE Trans. Power Syst., vol. 21, no. 2, pp. 916–924, May 2006.

[14]   Y. Li, D. M. Vilathgamuwa, and P. Loh, ―Design, analysis,   and   real-time testingofacontrollerformultibusmicrogridsystem, IEEETrans.Power Electron., vol. 19, no. 5, pp. 1195–1204, Sep. 2004.

[15]   C. L. Chen, Y. B. Wang, J. S. Lai, Y. S. Lai, and D. Martin, ―Design of parallel inverters for smooth mode transfer of microgrid applications,‖ IEEE Trans. Ind. Electron., vol. 25, no. 1, pp. 6–15, Jan. 2010.

[16]   S. Kouro, P. Cortes, R. Vargas, U. Ammann, and J. Rodr´ıguez, ―Model predictive control—A simple and powerful method to control power converters,‖ IEEE Trans. Ind. Electron., vol. 56, no. 6, pp. 1826–1838, Jun. 2009.

[17]   K. S. Low and R. Cao, ―Model predictive control of parallel-connected inverters for uninterruptible power supplies,‖ IEEE Trans. Ind. Electron., vol. 55, no. 8, pp. 2884–2893, Aug. 2008.

[18]

[18]J.RodriguezandP.Cortes,PredictiveControlPowerConve rtersElectrical Drives. Hoboken, NJ, USA: Wiley, 2012.

[19]   S. Mariethoz, A. Fuchs, and M. Morari, ―A VSC-HVDC decentralized model predictive control scheme for fast power tracking,‖ IEEE Trans.
Power Del., vol. 29, no. 1, pp. 462–471, Feb. 2014.

[20]   M. Korpas and A. Holen, ―Operation planning of hydrogen storage connected to wind power operating in a power market,‖ IEEE Trans.
Energy Convers., vol. 21, no. 3, pp. 742–749, Sep. 2006.

[21]   M. Falahi, S. Lotfifard, M. Eshani, and K. Butler-Purry ―Dynamic model predictive-based energy management of DG integrated distribution systems, IEEE Trans. Power Del., vol. 28, no. 4, pp. 2217–2227, Oct. 2013.

[22]   D.E.Olivares,A.Mehrizi-Sani,A.H.Etemadi,C.A.Ca˜nizares,R.Iravani et al., ―Trends in microgrid control, IEEE Trans. Smart Grid, vol. 5, no. 4, pp. 1905–1919, Jul. 2014.

[23]   N. Mendis, K. M. Muttaqi, S. Sayeef, and S. Perera, ―Standalone operation of wind turbine-based variable speed generators   with   maximum   powerextractioncapability, IEEETrans.EnergyConvers.,vol.27,no.4, pp.
822–834, Dec. 2012.

[24]   S. X. Chen, H. B. Gooi, and M. Q. Wang, ―Sizing of energy storage for microgrids,‖ IEEE Trans. Smart Grid, vol. 3, no. 1, pp. 142–151, Aug. 2011. [25] T. Dragicevic, J. M. Guerrero, J. C. Vasquez, and D. Skrlec, ―Supervisory control of an adaptive-droop

regulated DC microgrid with battery management capability,‖ IEEE Trans. Power Electron., vol. 29, no. 2, pp. 695–706, Feb. 2014.

[26]   M. Coleman, C. K. Lee, C. Zhu, and W. G. Hurley, ―State-of-charge determination from EMF voltage estimation: Using impedance, terminal voltage, and current for lead-acid and lithium-ion batteries, IEEE Trans. Ind. Electron., vol. 54, no. 5, pp. 2550–2557, Oct. 2007.

[27]   T. Kato, K. Tamura, and T. Matsuyama, ―Adaptive storage battery management based on the energy on demand protocol, in Proc. IEEE 3rd Int. Conf. Smart Grid Commun., 2012, pp. 43–48.

[28]L.XuandD.Chen,―ControlandoperationofaDCmicrogridwithvari able generation and energy storage, IEEE Trans. Power Del., vol. 26, no. 4,

pp. 2513–2522, Oct. 2011.

[29]   C. A. Hill, M. C. Such, D. Chen, J. Gonzalez, and W. M. Grady, ―Battery energy storage for enabling integration of distributed solar power generation, IEEE Trans. Smart Grid, vol. 3, no. 2, pp. 850–857, Jun. 2012.

[30]   O. Gomis-Bellmunt, A. Junyent-Ferre, A. Sumper, and J. Bergas-Jane,―Control of a wind farm based on synchronous generators with a central HVDC-VSC converter, IEEE Trans. Power Syst., vol. 26, no. 3, pp.

1632–1640, Aug. 2011.

[31]   W. Lu and B. T. Ooi, ―Optimal acquisition and aggregation of offshore windpowerbymultiterminalvoltage-sourceHVDC, IEEETrans. Power Del., vol. 18, no. 1, pp. 201–206, Jan. 2003.

[32]P.Cortes,G.Ortiz,J.I.Yuz,J.Rodriguez,S.Vazquez,andL.G.Franque lo, ―Model predictive control of an inverter with output LC filter for UPS applications,‖ IEEE Trans. Ind. Electron., vol. 56, no. 6, pp. 1875–1883, Jun. 2009.

[33]   L. Wang, Model Predictive Control System Design Implementation Using MATLAB, vol. 1. New York, NY, USA: Springer, 2009.